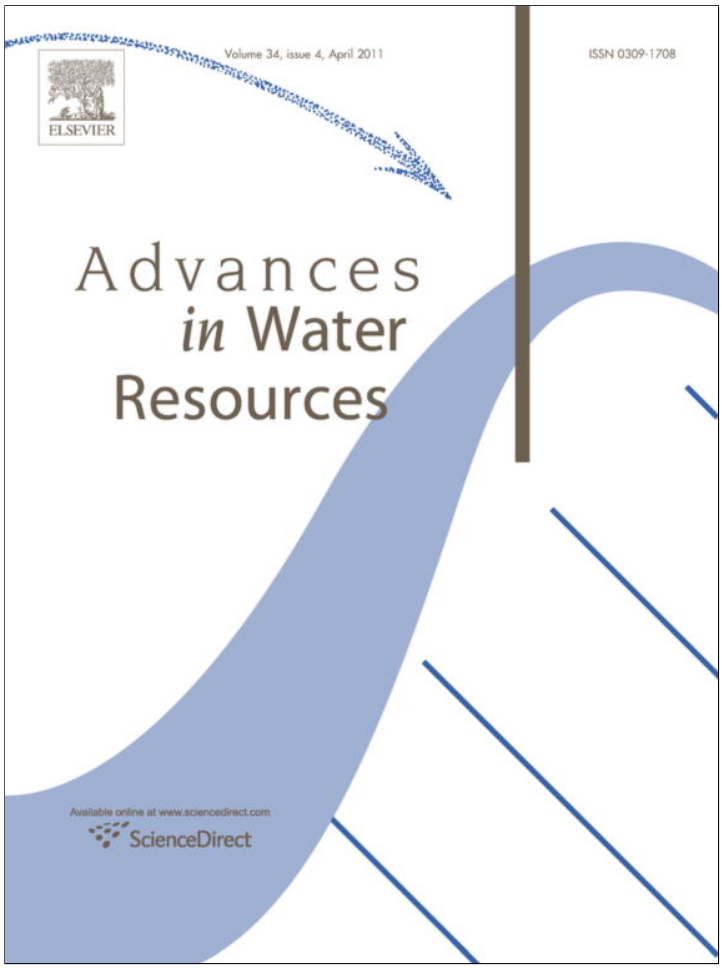

Advances in Water Resources 34 (2011) 526–536

Contents lists available at ScienceDirect

Advances in Water Resources

journal homepage: www.elsevier.com/locate/advwatres

Improving hydrologic predictions of a catchment model via assimilation of surface soil moisture

Fan Chen [a], Wade T. Crow [b,*], Patrick J. Starks [c], Daniel N. Moriasi [c]

[a] Science Systems and Applications, Inc./USDA ARS Hydrology and Remote Sensing Laboratory, Beltsville, MD 20705, United States
[b] USDA ARS Hydrology and Remote Sensing Laboratory, Beltsville, MD 20705, United States
[c] USDA ARS Grazinglands Research Laboratory, El Reno, OK 73036, United States

ARTICLE INFO

Article history:
Received 1 October 2010
Received in revised form 25 January 2011
Accepted 26 January 2011
Available online 4 February 2011

Keywords:
Soil moisture
Hydrologic modeling
Data assimilation
Remote sensing

ABSTRACT

This paper examines the potential for improving Soil and Water Assessment Tool (SWAT) hydrologic predictions of root-zone soil moisture, evapotranspiration, and stream flow within the 341 km^2 Cobb Creek Watershed in southwestern Oklahoma through the assimilation of surface soil moisture observations using an Ensemble Kalman filter (EnKF). In a series of synthetic twin experiments assimilating surface soil moisture is shown to effectively update SWAT upper-layer soil moisture predictions and provide moderate improvement to lower layer soil moisture and evapotranspiration estimates. However, insufficient SWAT-predicted vertical coupling results in limited updating of deep soil moisture, regardless of the SWAT parameterization chosen for root-water extraction. Likewise, a real data assimilation experiment using ground-based soil moisture observations has only limited success in updating upper-layer soil moisture and is generally unsuccessful in enhancing SWAT stream flow predictions. Comparisons against ground-based observations suggest that SWAT significantly under-predicts the magnitude of vertical soil water coupling at the site, and this lack of coupling impedes the ability of the EnKF to effectively update deep soil moisture, groundwater flow and surface runoff. The failed attempt to improve stream flow prediction is also attributed to the inability of the EnKF to correct for existing biases in SWAT-predicted stream flow components.

Published by Elsevier Ltd.

1. Introduction

Soil moisture plays an essential role in the exchange of energy and water within the soil–vegetation–atmosphere continuum. Successful initialization and modeling of soil moisture is crucial for the prediction of hydrologic processes including runoff, ground water recharge and evapotranspiration. Nevertheless, accurate estimation of soil moisture is typically limited by uncertainties in model inputs, parameter values and imperfect model physics regarding subsurface processes. Given the lack of a dense soil monitoring network in most regions, satellite observations are the most viable solution to improving the representation of soil moisture states in land surface and hydrologic models.

During the past decade a range of data assimilation techniques have been developed to optimally merge land model estimates with satellite observations to reduce modeling errors arising from various sources (e.g. [1–3]). At their core, these approaches provide a methodology for properly updating error-prone model predictions with incomplete and uncertain observations of model states. A variety of assimilation approaches have been proposed for this task. However, in recent years the Ensemble Kalman filter (EnKF) has emerged as (arguably) the most popular choice for land data assimilation. The EnKF is based on generating a Monte Carlo ensemble of model predictions in order to propagate the background uncertainty information required by the Kalman filter update equations (see Section 2.1 below for further details). Relative to competing approaches, the EnKF offers the benefits of easy implementation, flexibility regarding the nature of modeling error, computational efficiency and demonstrated robustness when applied to land surface models [4,5]. However, most hydrologic EnKF applications have focused on the estimation of soil moisture profiles and surface energy fluxes in land surface models used in numerical weather prediction. In contrast, relatively little data assimilation work has been conducted for rainfall-runoff and/or stream flow models commonly applied to water resource quantity and quality studies. The few studies that have been completed generally show some potential for improving runoff prediction by assimilating surface soil moisture and/or stream flow observations (e.g. [6–10]).

Studies examining the assimilation of surface soil moisture are highly relevant given the expected wealth of global soil moisture data products created by the current ESA Soil Moisture Ocean Salinity mission (SMOS) [11] and the upcoming NASA Soil Moisture

* Corresponding author.
E-mail address: Wade.Crow@ars.usda.gov (W.T. Crow).

0309-1708/$ - see front matter Published by Elsevier Ltd.
doi:10.1016/j.advwatres.2011.01.011

Active/Passive (SMAP) mission [12]. Both instruments will provide near-daily estimates of surface (0–5 cm) soil moisture – albeit at a relatively coarse spatial resolution of between 10 and 40 km. The ultimate value of these data products for improving water quality and quantity modeling is currently unknown.

The Soil and Water Assessment Tool (SWAT) is a physically-based, semi-distributed continuous watershed model developed to predict the impact of land management practices and climatic change on water, sediment and agricultural chemical yields over long periods of time [13,14]. SWAT has been widely applied to hydrologic (e.g. flow prediction, snow/runoff/groundwater/soil water dynamics, irrigation management) and water quality assessment (non-point source modeling, sediment yield, pollutant fate, best agricultural management practices, conservation effects) problems. Gassman et al. [15] provides a detailed review of the development and applications of SWAT. Despite its widespread and successful application to a number of critical water resources applications, SWAT is based on a much simpler representation of surface energy processes and the vertical redistribution of water within the soil column than land surface models used in past EnKF applications (see e.g. [16,17,2]). Given the importance of vertical processes that couple the surface to deeper model states in surface soil moisture data assimilation [18,19], it is unclear how effective existing land data assimilation techniques are when applied to SWAT. These issues must be addressed before SMOS and SMAP data products can be leveraged to enhance water resource applications currently addressed by SWAT modeling.

The objective of this study is to evaluate the potential of improving SWAT's hydrologic predictions (i.e. root-zone soil moisture, evapotranspiration, runoff and stream flow) within the 341 km^2 Cobb Creek Watershed in southwestern Oklahoma via the EnKF-based assimilation of surface soil moisture observations. The organization of this paper is as follows. Section 2 presents a review of the SWAT model and EnKF methodology, as well as details of the data used and a description of the design for the data assimilation experiments. Subsequent results are presented for two separate data assimilation experiments. Results in Section 3.1 are derived from a set of synthetic twin data assimilation experiments in which artificial observations are generated using the SWAT model. Results in Section 3.2 are analogous except for the more demanding case of assimilating actual soil moisture observations obtained within the Cobb Creek Watershed. Section 4 provides a brief summary and discussion of key results.

2. Methods and data

This section gives a brief description of the EnKF algorithm and summarizes basic SWAT physics with an emphasis on processes controlling runoff generation and the vertical redistribution of soil water. Methodologies for both the synthetic twin and real-data assimilation experiments are also presented.

2.1. Ensemble Kalman filter

As discussed above, the EnKF is a sequential data assimilation method evolved from the standard Kalman filter [20] that has been demonstrated to efficiently handle the assimilation of observations into moderately nonlinear models [5]. It is based on an ensemble generation of model states produced by adding Monte Carlo noise to model states and/or forcings to approximate the model forecast state error covariance matrix in order to optimally merge model predictions with observations.

Letting $Y(t)$ be a vector of background model states at time t and F a potentially non-linear land surface model, the continuous forecasting of $Y(t)$ via F can be expressed as:

$$\frac{dY(t)}{dt} = F[Y(t), w] \tag{1}$$

where the random noise term w represents the aggregate impact of modeling errors arising from various sources including: inadequate model physics, poorly calibrated parameters, and noisy forcing data.

Conversely, let Z_k be the observation vector collected at discrete time t_k and the observation process is derived as:

$$Z_k = M_k[Y(t_k)] + v_k \tag{2}$$

where M is the observation operator that relates the true state to the measured variable and v reflects the observation noise. The noise term v is assumed to be a mean-zero, Gaussian random variables with variance C_v and statistically independent of w.

The EnKF is based on minimizing the impact of w via the consideration of independent observations Z related to land surface states contained in Y. If F and M are linear and stated assumptions concerning v and w are met, then the optimal updating of Y replicates given the presence of an observation Z at time k can be expressed as:

$$Y_k^{i+} = Y_k^{i-} + K_k\left[Z_k + \varepsilon_k^i - M_k\left(Y_k^{i-}\right)\right] \tag{3}$$

where:

$$K_k = [C_{YM}(C_M + C_v)^{-1}]_{t=t_k} \tag{4}$$

and ε is a mean-zero, random variable independently sampled (for each ensemble member) from a mean-zero, Gaussian distribution with variance C_v (see [21]). Variables Y^{i+} and Y^{i-} in (3) are state vectors for the ith ensemble member before and after updating, respectively. K_k in (4) is the Kalman gain that defines the weights of measurement and model estimation and is calculated from the forecast error covariance matrix C_M of the measurement predictions $M_k[Y(t_k)]$ and the forecast cross covariance C_{YM} between any given state and $M_k[Y(t_k)]$. A single deterministic EnKF prediction (i.e. the "analysis") is then acquired by averaging model state predictions across the ensemble. The analysis of other model forecast variables (e.g. stream flow) is defined in the same manner.

2.2. Model description

SWAT is a physically-based, semi-distributed watershed model widely used to assess the impact of land management practices and climatic changes on long-term water, sediment and pollutant yields. A watershed is geographically delineated into a number of smaller sub-basins where flow routing is simulated. The sub-basins are further subdivided into hydrologic response units (HRU's) that consist of uniform land use, soil and management practices. While the area-fraction of a sub-basin covered by each HRU is accounted for, the exact location of each HRU is not explicitly represented. The HRU is a basic unit in SWAT where fundamental surface processes such as flow generation, soil water dynamics, crop growth, evapotranspiration, sediment and nutrient transport are simulated.

2.2.1. Flow generation

Total SWAT stream flow is calculated as

$$Q = Q_{surf} + Q_{lat} + Q_{gw} \tag{5}$$

where Q is total stream flow of the day (mm H_2O), Q_{surf} is surface runoff (mm H_2O), Q_{lat} is subsurface lateral flow (mm H_2O) and Q_{gw} is groundwater flow (mm H_2O). Surface runoff, lateral flow and groundwater flow are generated from each HRU and aggregated at the main channel of each sub-basin, then routed to obtain the total stream flow for the watershed.

Surface runoff (Q_{surf}) is estimated using the Soil Conservative Service (SCS) curve number procedure:

$$Q_{surf} = \frac{(R_{day} - 0.2S)^2}{R_{day} + 0.8S} \tag{6}$$

where R_{day} is daily precipitation (mm H_2O) and S a retention parameter defined as:

$$S = 25.4\left(\frac{1000}{CN} - 10\right). \tag{7}$$

In (7), CN is the curve number for the day, which is a function of the input parameter $CN2$ (initial curve number at average moisture condition) and initial soil profile water content of the day (mm H_2O) excluding the amount of water held at wilting point. Further details concerning the relationship between soil moisture and CN are available in [14].

Subsurface lateral flow occurs when a soil layer is saturated in a sloped HRU:

$$Q_{lat} = \sum_{ly=1}^{m} \frac{0.048 \cdot (SW_{ly} - FC_{ly}) \cdot K_{sat,ly} \cdot slp}{(\phi_{soil,ly} - \phi_{fc,ly}) \cdot L_{hill}} \tag{8}$$

where Q_{lat} is the total lateral flow from an HRU for the day (mm H_2O), ly is the soil layer, m is the total number of soil layers in the profile, SW_{ly} is the soil water content of the layer (mm H_2O), FC_{ly} is the water held at field capacity (mm H_2O), $K_{sat,ly}$ is the saturated hydraulic conductivity (mm/h), slp is the slope steepness (m/m), $\phi_{soil,ly}$ is the total porosity of the soil (mm^3/mm^3), $\phi_{fc,ly}$ is the VSM of the soil at field capacity (mm^3/mm^3), and L_{hill} is the slope length (m). The subscript $_{ly}$ indicates a layer-specific parameter.

In this study we use the term event flow (Q_{evt}) to represent the combined surface and near-surface contribution to total stream flow in response to a storm event:

$$Q_{evt} = Q_{surf} + Q_{lat}. \tag{9}$$

When the amount of water stored in the shallow aquifer is greater than the threshold water level, groundwater flow is generated:

$$Q_{gw,i} = Q_{gw,i-1} \cdot \exp[-\alpha_{gw}] + w_{rchrg} \cdot (1 - \exp[-\alpha_{gw}]) \tag{10}$$

where $Q_{gw,i}$ and $Q_{gw,i-1}$ represent groundwater flow into the main channel on day i and $i-1$ (mm H_2O) respectively, α_{gw} is the base flow recession constant, and w_{rchrg} is the amount of recharge entering the shallow aquifer on day i (mm H_2O).

2.2.2. Soil water dynamics

Soil moisture plays a central role in SWAT's simulation of various hydrologic processes such as runoff and lateral flow generation, evapotranspiration and groundwater recharge. Water entering the SWAT soil profile is redistributed using a storage routing technique that simulates water flow through each soil layer in the root zone at the HRU scale on a daily basis. The water balance equation for each layer can be expressed as:

$$SW'_{ly} = SW_{ly} + \Delta w_{perc,ly} - w_{lat,ly} - E_{a,ly} \tag{11}$$

where SW'_{ly} is the soil water content (mm H_2O) at the end of the day, SW_{ly} is the initial soil water content (mm H_2O), $\Delta w_{perc,ly}$ is the net percolation received in the layer (i.e. percolation from the overlaying layer or infiltration from land surface minus percolation to the next layer) (mm H_2O), $w_{lat,ly}$ is the lateral flow leaving the layer as calculated in Eq. (8), and $E_{a,ly}$ is the evapotranspiration drawn from the layer during the day (mm H_2O).

The amount of infiltration into the surface layer is the difference between R_{day} and Q_{surf} in (6). Percolation from each layer is then calculated as:

$$w_{perc,ly} = (SW_{ly} - FC_{ly}) \cdot \left(1 - \exp\left[\frac{-24 \cdot K_{sat,ly}}{SAT_{ly} - FC_{ly}}\right]\right) \tag{12}$$

where $w_{perc,ly}$ is the seepage from a layer at the end of the day, SAT_{ly} is the amount of water in the layer when completely saturated (mm H_2O) and other terms are previously defined. The percolation generated from bottom layer is the source for ground water recharge.

The vertical transfer of soil moisture in unsaturated layers is largely controlled by the evapotranspiration process. First, potential evapotranspiration (PET, mm H_2O) is calculated using the Penman–Monteith equation [22]. Potential soil water evaporation (E_s, mm H_2O) is a function of PET and leaf area index. Potential plant uptake (E_p, mm H_2O) is also estimated using the Penman–Monteith equation. Using depth distribution functions, potential E_s and E_p are determined for each soil layer (for details, see [14]. Actual soil water extraction is constrained by available water in a given layer and is not allowed to be compensated by extraction from another layer. However, users can adjust the parameters $ESCO$ (soil evaporation compensation factor, dimensionless) and $EPCO$ (plant uptake compensation factor, dimensionless) to modify the depth distribution of potential E_s and E_p. Both $ESCO$ and $EPCO$ have a range between 0 and 1.00. As $ESCO$ approaches 0 (or $EPCO$ approaches 1.0), more soil evaporative demand (or plant uptake demand) can be met by deeper layers. When $EPCO$ is set to zero, 50% of the water uptake will occur in the upper 6% of the root zone [14]. Actual evapotranspiration (AET, mm H_2O) also includes contributions from other minor sources such as ice/snow sublimation and evaporation from water bodies and wet canopy.

2.3. Site description and input data

The Cobb Creek Watershed covers a 341.56 km^2-area in southwestern Oklahoma in Caddo, Washita and Custer counties (Fig. 1). Land use in the watershed is approximately 56% in cropland (~90% of which is winter wheat with the rest in cotton, grain sorghum and peanut), 41% in pasture and 3% miscellaneous (forest/water/urban). Most soils are sandy clays and loams. It is a sub-watershed of the Fort Cobb Reservoir Watershed where annual precipitation and potential evapotranspiration are approximately 820 and 1850 mm, respectively [23]. Irrigation is limited to summertime periods when crops are stressed.

Daily meteorological data (precipitation, maximum/minimum temperatures, solar radiation, wind speed and relative humidity) are provided by three Oklahoma Mesonet stations: Fort Cobb (35° 8′ 55″ N, 98° 27′ 57″ W), Hinton (35° 29′ 3″ N, 98° 28′ 53″ W) and Weatherford (35° 30′ 29″ N, 98° 46′ 30″ W) located in the vicinity of the watershed. *In situ* soil moisture monitoring is available from a dense weather station network (i.e. the ARS Micronet) operated by the USDA Agricultural Research Service's (ARS) Grazinglands Research Laboratory since July 2005 in the Fort Cobb Reservoir Watershed. Data from seven stations located within or in the vicinity of the Cobb Creek Watershed is used in this study (Fig. 1). Soil moisture measurements are taken at 30-min intervals at 5-, 25- and 45-cm depths with Stevens Hydra Probes.[1] Daily flow discharge is measured at a US Geological Survey stream flow gauge located at the outlet of the watershed (07325800, Cobb Creek near Eakly) since 1969. For details on other model inputs (e.g. topography, management, soil physical properties) refer to [24]. Based on the DEM, land use and soil data, the watershed is divided into 43 sub-basins and 512 HRU's for SWAT modeling.

2.4. Model calibration

SWAT was calibrated using recorded daily stream flow of 2006–2008 at the outlet of the Cobb Creek Watershed. Parameter optimization was based on the integrated SCE-UA (shuffled complex

[1] Mention of particular commercial product does not imply endorsement by the USDA.

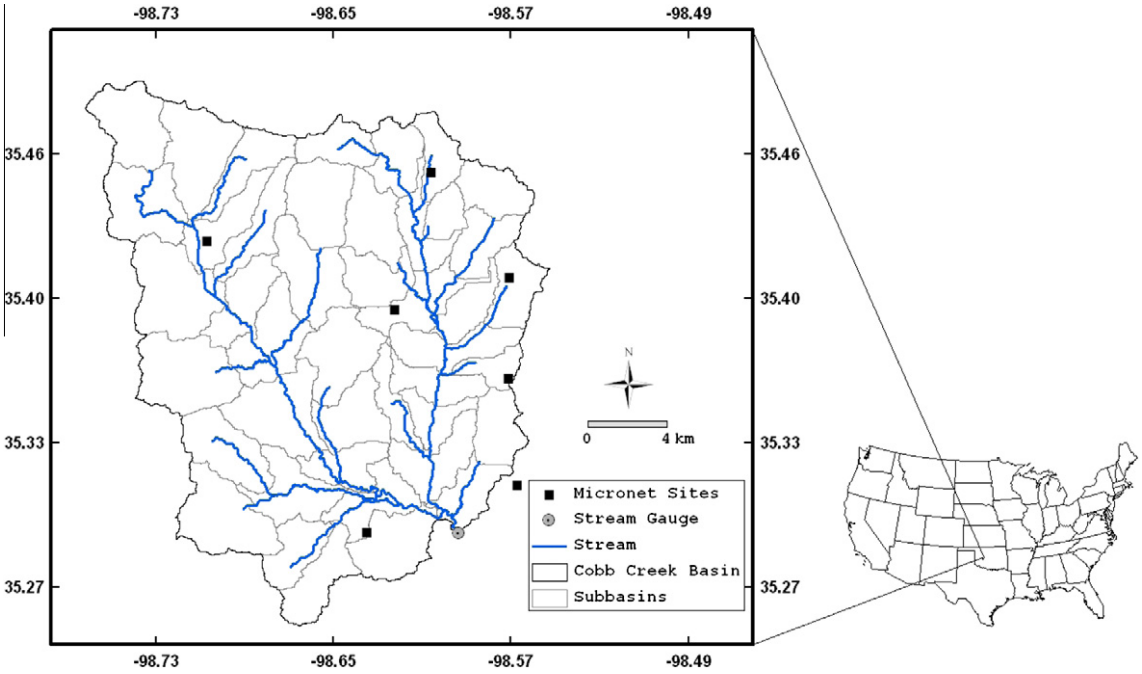

Fig. 1. Map of Cobb Creek Watershed and locations of soil water and stream flow monitoring sites.

evolution method developed at the University of Arizona) algorithm [25] through the minimization of the root-mean-square misfit of model total stream flow predictions to observations. Note that this choice of metric tends to emphasize the fitting of stream flow peaks at the expense of correcting bias during low-flow periods. Possible consequences of this tendency are discussed in Section 4 below.

Prior to calibration, a sensitivity analysis was performed to determine the following parameters to be optimized: *CN2*, *ESCO*, *EPCO*, K_{sat}, *Sol_AWC* (available water capacity, mm/mm) and *SURLAG* (surface runoff lag time, days). *CN2*, *ESCO*, *EPCO*, K_{sat}, have been previously defined. *Sol_AWC* is a layer-specific parameter describing the maximum water that can be held in a soil layer between saturation and wilting point. *SURLAG* is used to determine the portion of surface runoff that reaches the main channel of a sub-basin when the time of concentration is greater than one day. As *SURLAG* decreases, more water is held in storage and the amount of water reaching the sub-basin outlet decreases. Initial *ESCO*, *EPCO* and *SURLAG* were changed to fixed values for the entire watershed whereas distributed (i.e. HRU-specific) values of *CN2*, K_{sat} and *Sol_AWC* were adjusted by calibrated ratios. Calibrated values of these parameters are listed in Table 1.

2.5. EnKF implementation

The EnKF was based on generating an ensemble of SWAT realizations within each daily time step. The ensemble was created by adding random perturbations to SWAT forcing fields (i.e. precipitation and air temperature) and predicted soil moisture states to represent the modeling errors *w* in (1). Daily watershed-scale precipitation perturbations were generated by multiplying observed precipitation by a log-normally distributed, unit mean, spatially homogeneous and temporally uncorrelated random noise with a 0.2-mm standard deviation. In addition, a normally distributed, zero mean, spatially homogeneous, temporally uncorrelated noise with a 1.0-K standard deviation was added to both daily maximum and minimum air temperatures. The perturbations applied directly to SWAT soil moisture states were normally distributed, zero mean with a lag-1 (i.e. 1-day time gap) autocorrelation of 0.5 and a standard deviation of 0.05, 0.02, 0.02 and 0.01 m^3/m^3 per day from the top to bottom layer, respectively. The perturbations are spatially uniform, i.e. the exact same perturbation was applied to all HRU's on any given day. Vertical error correlations of both 0.0 and 1.0 were examined for our synthetic as well as real-data assimilation experiments (see Section 3).

The state vector *Y* in (1) and (3) was assumed to contain predictions for all vertically discrete SWAT soil moisture states. Since the size of individual HRU's is considerably smaller than a typical resolution of satellite-based surface soil moisture retrievals (>10 km), *M* in (2) was defined as an area-weighted average operator which maps surface soil moisture within individual HRU's into a single watershed average prior to its comparison with a watershed-scale surface soil moisture observation. The gain matrix *K* in (3) was then used to map the results of this comparison back to the spatially-varying state space within each individual HRU. In SWAT, VSM was regarded as being vertically constant within a given layer.

An additional complication is the lack of uniform soil layer depths between HRU's, which makes it difficult to obtain the forecast cross covariance term C_{YM} in (4). To simplify the updating process, soil profiles across the watershed were temporarily resampled into four consistent vertical layers with the bottom depths of 3, 30.5, 130 and ~180 cm respectively. When a day's

Table 1
Initial and calibrated SWAT parameters.

	CN2	*Sol_AWC* (mm/mm)	K_{sat} (mm/h)	*ESCO*	*EPCO*	*SURLAG* (days)
Initial	36–77	Vary	Vary	0.95	1	4
Calibrated	+5.7%	+25%	+24%	0.83	0.12	0.16

hydrologic simulations were completed, predicted VSM for each of these four pseudo-layers were used to obtain the Kalman gain and updated accordingly. Updated soil water values were then re-sampled back into original soil layers of each HRU prior to the start of the next day's SWAT simulation step.

2.5.1. Synthetic twin methodology

Synthetic twin experiments were performed to examine the EnKF's ability to improve SWAT's hydrologic modeling results when the exact error characteristics of the model and observations were assumed known. The truth run in these experiments was simply the trajectory of a SWAT model simulation without any perturbations. The observation to be assimilated by the EnKF runs (i.e. Z in (2)) was a single daily value obtained by taking the area-weighted spatial average of the top-layer (3-cm) VSM of the truth run degraded via the additive introduction of temporally-uncorrelated noise sampled from a mean-zero Gaussian distribution with a 0.03 m^3/m^3-standard deviation. Next an "open loop" run was generated by applying both forcing and model perturbations to a single SWAT model realization. In the EnKF run, we created a 50-member ensemble of realizations with stochastic forcing and model errors (using the same statistical behavior as in the open loop run) on top of the open loop perturbations. Past work has indicated that an ensemble of this size is appropriate for the application of the EnKF to this general class of land data assimilation problems [8,26]. The error covariance of the observations (C_v) applied in the EnKF was assumed to be perfectly known (i.e. equal to the square of the standard deviation of the mean-zero, Gaussian noise distribution used to generate the synthetic observations).

This ensemble was then updated using the synthetically generated (and degraded) observations and the EnKF approach outlined in Section 2.1. To dampen spurious variations in EnKF results due to initialization of the procedure with different random number sequences, twenty separate paired open loop and EnKF runs were conducted. Synthetic EnKF predictions were then evaluated relative to predictions acquired from the original SWAT truth run and reported results based on averaging evaluation metrics (see Section 2.6) across the twenty separate EnKF experiments.

2.5.2. Real data methodology

In addition to the synthetic data assimilation experiment described above, the availability of dense ground soil moisture measurements within the Cobb Creek Watershed allows for the assimilation of real surface soil moisture observations and the subsequent evaluation of EnKF results using independent soil moisture profile and stream flow measurements. Such real data approaches provide a more realistic assessment of assimilation potential than idealized synthetic experiments. Relative to a synthetic experiment, a real data assimilation analysis requires different approaches (detailed below) for generating the open loop simulation and preparing observational data.

In order to simulate the spatial resolution of a typically satellite-based soil moisture product, daily 5-cm VSM measurements from seven Micronet sites (see Fig. 1 and Section 2.3) were spatially averaged into a single daily value for the entire watershed. The weight given to each station during spatial averaging was proportional to the area of watershed enclosed by the Thiessen polygon centered upon each station. Potential sampling bias could result from the fact that all Micronet sites are located on native and improved grass and other land cover types were not sampled, especially during June–September when the winter wheat fields that cover about half of the watershed were fallow for tillage operations. However, since the watershed is mostly in rain-fed grain fields and pasture, these observations were regarded as representative of the watershed's spatially-averaged condition for most of the year. Soil moisture observations based on the averaging of ground-based Micronet observations were not further degraded via introduced noise to reflect remote sensing retrieval uncertainty. In addition, a single observation per day was assumed which is somewhat higher than the observational rate (four retrievals every 5 days) currently available at mid-latitudes by combining ascending and descending satellite overpasses. Therefore, real data EnKF results should be interpreted as a best-case scenario for the assimilation of a remotely-sensed surface soil moisture product into SWAT.

In real-data assimilation experiments, the control simulation, also referred to as the "open loop", was the unperturbed model realization without data assimilation. The update simulation (i.e. the EnKF run) used a 200-member ensemble and was updated via the EnKF procedure described in Section 2.1. To eliminate the systematic bias between observations and model predictions, daily observation were linearly rescaled so that their long-term mean and standard deviation match those of the multi-year model estimation:

$$\theta'_{o,i} = (\theta_{o,i} - \overline{\theta_o})\frac{\sigma_{\theta_o}}{\sigma_{\theta_s}} + \overline{\theta_s} \tag{13}$$

where $\theta_{o,i}$ is the observed surface VSM of day i, θ_s is SWAT-simulated surface VSM and the overbars indicate long-term temporal averaging. Variables σ_{θ_o} and σ_{θ_s} are the temporal standard deviations of observed and simulated surface VSM, respectively. Limited by the length of observation and period of model calibration, 2006–2008 data for both θ_o and θ_s were used. After the application of (13), the resulting rescaled soil moisture product was used for the EnKF observation Z in (2) and (3).

Modeling errors were assumed to be identical to those used in the synthetic data assimilation experiment and the vertical error correlation between the surface and other deeper layers were set to be 1.0. We also experimented with zero-vertical error correlation which resulted in poorer analysis outcome (not shown). Here the surface layer in SWAT was defined as the top 5 cm of the soil column to match the expected observation depth of a microwave sensor. Although only surface soil moisture was being assimilated, the availability of VSM measurements at 25 and 45 cm and the layer-by-layer output of SWAT allows us to evaluate EnKF performance at each layer with a crude assumption which regarded observed 5, 25 and 45 cm VSM's as adequately representing VSM within the top three SWAT soil layers. EnKF performance was also evaluated for an aggregated root-zone layer, which referred to the combination of the top three layers. During the application of the EnKF, the error covariance of the observations (C_v) was assumed equal to 0.03^2 m^6/m^6.

EnKF results were also evaluated based on comparisons to basin-outlet stream flow (see Section 2.3) and observed groundwater flow obtained as average of the first two filter passes generated by processing observed stream flow through the Base Flow Separation Program [27]. Event flow was the difference between total stream flow and estimated groundwater flow. As in the synthetic case described above, the model forecast ensemble is created by applying model and forcing perturbations described in Section 2.5. However, unlike the synthetic case, there is no guarantee that these perturbations accurately reflect true modeling error. The impact of this potential error source on real data assimilation results is discussed at the end of Section 3. All experiments (both synthetic and real data) were run for four calendar years (2005–2008). Calendar year 2005 was used as a spin-up period, and the assimilation of observation began on January 1, 2006.

2.6. Evaluation metrics

Since it is difficult to compare the skill improvement of EnKF across model prognostic variables with different units, a normalized error reduction (NER) index was calculated as:

$$NER = 1 - \frac{RMSE_a}{RMSE_o} \tag{14}$$

where $RMSE_o$ and $RMSE_a$ are the root-mean square errors for the open loop and the analysis, respectively. NER has a value between negative infinity and 1.0. For a negative NER, the assimilation results in deteriorated states/fluxes compared to the open loop. As NER approached 1.0 data assimilation realizes greater improvements over the open loop. Multiplying NER by 100 gives the percent reduction of open loop RMSE.

Percent bias (Pbas) was used to assess the long-term simulated bias relative to observed/true values:

$$Pbas = 100 \cdot \left(\frac{\sum_{i=1}^{n} x_{s,i}}{\sum_{i=1}^{n} x_{o,i}} - 1 \right) \tag{15}$$

where $x_{s,i}$ is the simulated value of variable x for day i, $x_{o,i}$ is the observed/true value of day i and n is total number of days simulated.

The Nash–Sutcliffe efficiency index (NSE) was used to assess the goodness-of-fit for hydrologic predictions to observations [28]:

$$NSE = 1 - \frac{\sum_{i=1}^{n} (x_{s,i} - x_{o,i})^2}{\sum_{i=1}^{n} (x_{o,i} - \overline{x_o})^2} \tag{16}$$

where $x_{s,i}$, and $x_{o,i}$ are previously defined and $\overline{x_o}$ is the mean of observed/true value of x. One advantage of the Nash–Sutcliffe index is that it can be applied to nonlinear models and therefore it is widely used in evaluating hydrologic models [29]. NSE ranges from negative infinity to 1.0. Moriasi et al. [30] provided guidelines for performance ratings using NSE as "very good" ($0.75 > NSE \leq 1.0$), "good" ($0.65 > NSE \leq 0.75$), "satisfactory" ($0.50 > NSE \leq 0.65$) and "unsatisfactory" ($NSE \leq 0.50$) for a monthly time step. For a daily time step lower thresholds should be used.

3. Results

As discussed above, our analysis encompassed both an initial synthetic study (described in Section 3.1) to examine the feasibility of an EnKF under optimal circumstances and a real-data experiment (described in Section 3.2) where actual ground-based soil moisture observations were assimilated into the SWAT model.

3.1. Synthetic twin data assimilation experiments

In the synthetic experiments, the "truth" was assumed to be an unperturbed SWAT realization and the "open loop" was a SWAT simulation perturbed by adding prescribed Gaussian errors to the model (see Section 2.5.1). The "EnKF run" corrected the open loop (back to the truth simulation) by assimilating surface soil moisture information generated from the truth run and artificially degraded with added synthetic observation errors. Since the seed of a particular random number generator can produce a unique set of synthetic results for each realization of the system, reported evaluation metrics were based on average values obtained from 20 separate open loop and/or EnKF realizations – each based on a unique seeding of a Gaussian random number generator.

3.1.1. Impact of error coupling

Past work has demonstrated that the impact of assimilating surface soil moisture retrievals is sensitive to the magnitude of vertical correlation within EnKF perturbations w applied directly to soil moisture within various model layers [19]. Since the covariance of w is arbitrary specified in a synthetic experiment, the impacts of vertical correlation in applied soil moisture perturbations can be directly examined. For SWAT, Fig. 2 presents the spread of NER for major hydrologic states and fluxes (defined in Section 2.2) within twenty independent EnKF realizations for the cases of both perfect vertical error correlation (i.e. a correlation of one between perturbations applied to each layer) and zero vertical error correlation.

For the zero-vertical error correlation case, assimilating surface soil moisture led to large improvement for soil moisture within top two pseudo-layers (see Section 2.5), eliminating nearly 60% of the open loop error. However, much lower levels of NER were seen for the bottom two layers. For profile soil water content (SW) and AET, open loop errors were reduced by about 20%. NER varied in a narrow range for soil moisture, AET, and Q_{lat}, indicating consistent effectiveness of EnKF on these variables regardless of how the open loop is initialized. However, for other flow-related variables, large realization to realization differences were seen in the performance of the EnKF. With the exception of Q_{gw}, the distribution of NER from across 20 runs was nearly symmetric (i.e. similar mean and median values) for all variables. For those variables with some negative NER values, positive median values indicated that they received improvement in half or more runs.

In most EnKF runs, stream flow (Q) received moderate improvement, largely associated with improved event flow (Q_{evt}) which contributed nearly 85% of the total Q. Of the Q_{evt} components, both surface runoff (Q_{surf}) and subsurface lateral flow (Q_{lat}) were improved; however, improvements to Q_{lat} were more consistently observed. This can be related to the fact that Q_{lat} was mostly

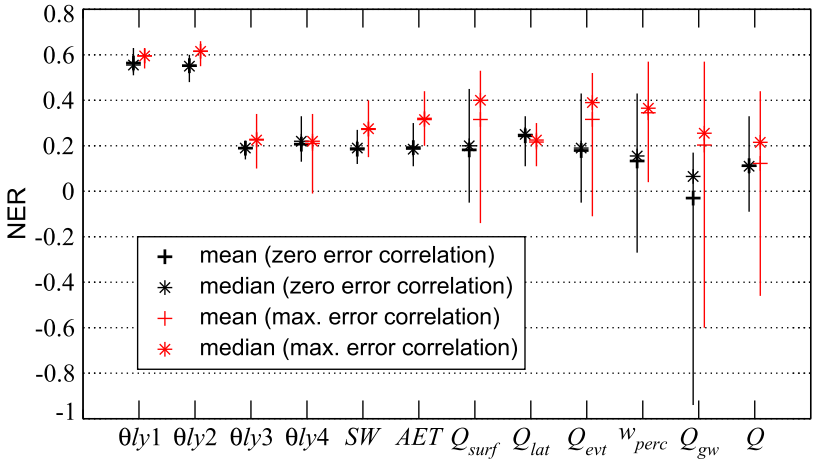

Fig. 2. The NER of SWAT states and fluxes as a result of twenty repeated experiments with either zero or maximum vertical error correlation. Vertical error bars indicate data ranges. Higher NER indicates greater improvement upon assimilation. The first four variables (left to right) are soil moisture in the top four soil layers. See Section 2.2 for the definition of other plotted states and fluxes.

generated from the top soil layers that received the greatest improvement upon the assimilation of surface soil moisture observations while Q_{surf} was constrained by the total profile soil water (which only experiences a modest improvement upon assimilation). Since deep percolation is the sole source of groundwater in SWAT, improvement in w_{perc} generally leads to analogous improvement in Q_{gw}. Degraded Q_{gw} cases were found to be associated with worse EnKF performance in w_{perc} (i.e. larger negative bias than the open loop) during the rainy period of summer 2007. Due to the highly autocorrelated nature of Q_{gw}, this resulted in a sustained period of underestimated Q_{gw}. Therefore in 3 out of 20 cases, deterioration in EnKF Q_{gw} was observed even with improved long-term w_{perc} and, in one case, amplified Q_{gw} degradation (NER of -0.45) was observed with deteriorated w_{perc} (NER of -0.27).

Generally larger improvement was noted for EnKF results when the vertical correlation of soil moisture perturbations was maximized as one (Fig. 2). Nevertheless, the magnitude of improvement was always smaller for bottom soil layers and only slightly larger for profile soil water and *AET* predictions. More significant improvements were noted for flow-related variables (e.g. Q_{surf}, w_{perc} and Q_{gw}) than the zero-vertical error correlation case discussed above. However, it is worth clarifying that in addition to affecting the performance of the EnKF analysis, variations in vertical error correlation assumptions also impacted the amount of error in the open loop simulation. Therefore, since NER only suggests the amount of correction relative to the open loop, a higher value does not automatically guarantee superior analysis (i.e. a lower RMSE) compared to the truth. For example, assuming high error correlation yielded greater NER for w_{perc}, but the corresponding EnKF RMSE was actually larger than the low error correlation case (not shown). This was also true for some other variables (e.g. the VSM of the bottom soil layer, *SW*, *AET*, Q_{surf} and *Q*). For our synthetic experiments, assuming zero vertical error correlation generally yielded better soil moisture and stream flow RMSE results despite having lower NER than the maximum-error correlation case.

3.1.2. Impact of vertical coupling strength

As noted in [18,19], variations in model vertical coupling can also impact prospects for constraining lower-layer soil moisture based on the assimilation of surface soil moisture observations. To test the effectiveness of the EnKF on SWAT hydrologic predictions with different vertical coupling strengths, we conducted two experiments with different combinations of extreme *ESCO*/*EPCO* values. These two variables were selected because they have a direct impact on the degree of SWAT vertical soil water coupling. As *ESCO* decreases and *EPCO* increases, more soil evaporative and plant uptake demand can be drawn from deeper layers when the demand cannot be met by the upper layers (see Section 2.2). Therefore, the *ESCO*/*EPCO* values effectively control the degree to which soil moisture of lower layers varies according to the availability of soil water in upper layers and hence the vertical moisture coupling within the modeled soil profile. The amount of SWAT vertical coupling could also vary as a function of site-specific soil properties, especially K_{sat}. However, since soil water redistribution in SWAT is sensitive to K_{sat} only during brief periods in which soil water content is above field capacity, we have held it constant here and instead focused on the impact of more widely relevant *ESCO* and *EPCO* variations.

In the first experiment (“Maxcoup”) the *ESCO* and *EPCO* values were set to 0.01 and 1.00 respectively, which allowed evaporative demand to be met from the maximum depth possible. The second experiment (“Mincoup”) used *ESCO* and *EPCO* values of 1.00 and 0.01, respectively, to restrict evapotranspiration to a thin layer near the surface. Two separate truth trajectories were generated using the above mentioned *ESCO*/*EPCO* values with other parameter values fixed, and twenty separate EnKF assimilation runs were performed for each case. For these new experiments, vertical error coupling was set to be zero.

Table 2 shows the coupling strength between surface and underlying layers obtained from the truth runs of the Maxcoup and Mincoup cases. The vertical coupling strength of SWAT-predicted soil moisture was assessed by the Pearson product–moment correlation coefficient between the VSM time series of two different layers. The correlations between the surface and layers 3 and 4 were extremely low in the Mincoup experiment (0.16, 0.01). Corresponding coupling strengths for the Maxcoup case were only marginally greater (0.29, 0.17). As a result of this modest change in coupling strength, the Maxcoup experiment exhibited only slightly better data assimilation skill in the bottom layer than the Mincoup experiment (Fig. 3). This lack of variation suggests that the subsurface physics of SWAT results in generally weak vertical soil water coupling, and therefore weak EnKF updating of subsurface soil moisture states, regardless of the parameterization chosen for root-water extraction.

On the other hand, the choice of root-water extraction parameters did make a difference in other SWAT flux variables. Since water uptake by evapotranspiration was restricted to the upper layers where improvement was greatest, the Mincoup experiment showed considerably better skill in *AET*. In general, the Maxcoup experiment showed greater case-to-case variability for flow-related variables, likely due to their smaller absolute volume. By allowing more extraction from the lower depths, substantially higher *AET* was generated and the soil profile was generally drier. This led to reduced runoff and severely reduced ground water recharge and hence substantially lower amounts of total *Q*. Reductions to *Q* were primarily concentrated in the Q_{evt} component that contributes about ~95% of the total flow volume in the Maxcoup case. Because of the predominance of Q_{evt} in *Q*, NER of *Q* was heavily impacted by the ENKF performance during major storm events. When, during certain storm events, the EnKF run had larger biases of the same sign in both Q_{evt} and Q_{gw} than the open loop, *Q* exhibited worse NER than its component variables (Fig. 3). The Mincoup case, on the other hand, evaporated much less and generated greater amounts of *Q*. Although SWAT soil moisture predictions were virtually decoupled vertically, total stream flow was consistently improved because of improved event flow which contributes about ~75% of total flow by volume (in the Mincoup case). Different results would be expected for basins where Q_{gw} makes up a greater portion of total stream flow.

In a crude sense, the *ESCO*/*EPCO* values used in the Maxcoup experiment are applicable for regions of higher hydraulic conductivity (K_{sat}) and/or deep-rooted vegetation. In our study site where pasture and annual crops constitute the major land cover, maximum root density is relatively shallow and soil water is primarily drawn from the upper layers. This is reflected by the calibrated *ESCO*/*EPCO* values (0.86, 0.12) being relatively closer to the Mincoup case. As noted above, SWAT vertical coupling may also be impacted by parameters not considered here, and the overall impact of coupling might result from the complex interaction of multiple parameters. Therefore the above experiments were highly simplified and should be considered only preliminary. Nevertheless, the

Table 2
The Pearson correlation coefficient between various SWAT soil moisture layers for the Maxcoup and Mincoup experiments.

	Maxcoup			Mincoup		
	Layer 2	Layer 3	layer 4	Layer 2	Layer 3	layer 4
Layer 1	0.93	0.29	0.17	0.92	0.16	0.01
Layer 2		0.38	0.24		0.22	0.06
Layer 3			0.94			0.96

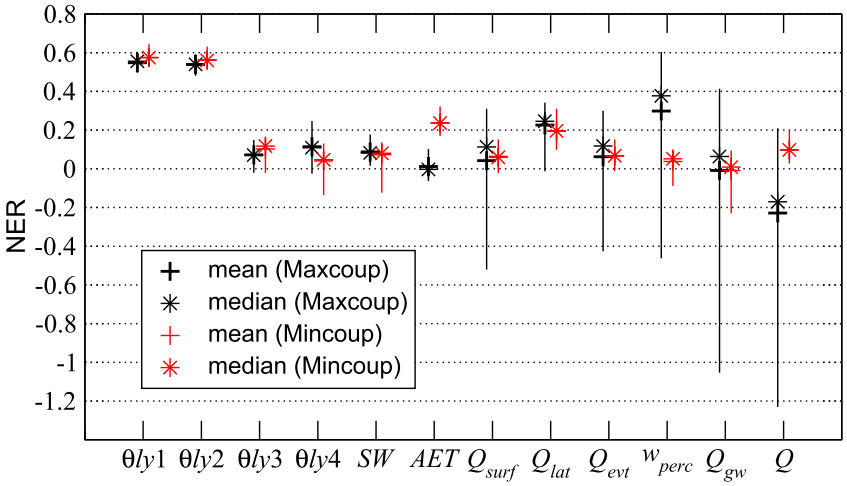

Fig. 3. Same as Fig. 2 for the Maxcoup and Mincoup experiments.

results suggested that the ultimate source of limited success in constraining deep layer soil moisture (and subsequently percolation and base flow) was SWAT's model physics, not our particular choice of root-water extraction parameters.

3.2. Real-data EnKF experiment

In the real-data EnKF experiments, spatial-averaged ground observations of 5-cm VSM were assimilated with an assumed modeling error correlation of 1.0 between surface and lower layers. This experiment provided a more challenging test for an EnKF since, in a real data environment, the actual error characteristics of the model are unknown and there is no assurance that such characteristics match the assumptions underlying the EnKF [31]. In addition, real data assimilation results are often degraded by uncertainties in the data sets used for evaluation purposes.

Time series of observed, open loop and EnKF soil moisture and stream flow values are shown in Figs. 4 and 5, respectively, for the real-data EnKF case. Root zone referred to the top three layers combined which encompassed the entire soil profile from the surface to a depth of 130 cm. Not surprisingly, comparisons with actual ground-based observations revealed relatively less marginal improvement than comparable results obtained in synthetic experiments described above (Fig. 6). Difficulties in real data cases were particularly acute when modeling error manifested itself as a bias. Persistent positive bias in root-zone soil moisture was found in the open loop and was most pronounced in the third (45-cm) soil moisture layer (Fig. 4c). As previously discussed, the calibrated *ESCO*/*EPCO* values used in the SWAT open loop indicated that most simulated evapotranspiration was drawn from a relatively thin soil layer near the surface. This means less involvement of lower layers in the evapotranspiration process and the effective decoupling of deeper soil moisture from surface dynamics, which also explains the damped temporal variation of SWAT 45-cm soil moisture predictions relative to observations.

Although calibration has been targeted for stream flow instead of soil moisture, the outcome of the Maxcoup experiment (Section 3.1.2) suggests that the lack of vertical coupling in SWAT is a model structural, rather than parametric, problem. Similar to the synthetic experiment results, there was greater relative EnKF improvement in the soil moisture states in the top two layers than the deeper layers (Fig. 4). However, improvement was moderate in scope for the top layers and only marginal for lower layers. Because the surface VSM observation was scaled to the climatology of SWAT soil moisture predictions prior to assimilation and the weak vertical coupling noted above, the EnKF was unable to correct for the presence of bias in lower soil moisture layers. Nevertheless, assimilating the surface observation led to increased temporal variability in the root-zone soil moisture which is in better agreement with observations (Fig. 4d).

Table 3 presents the simulated and actual vertical coupling strengths within the top three layers varied by actual surface wetness in further detail. For each case (observation, open loop or EnKF), "wet" or "dry" conditions referred to days on which top 5-cm soil moisture was above or below the average of the particular time-series. Under dry surface conditions, observed vertical coupling strength was similar to the all-time conditions, while it was much weaker in the wet surface conditions. The lack of coupling in wet conditions is attributable to relatively low demand for plant water uptake that is largely drawn from the upper layers in the wet surface conditions. In drier conditions root uptake from deeper layers increases and the available water in the upper layer affects the amount of extraction from below. Nevertheless, relatively large amount of vertical coupling was consistently found within the soil moisture observations.

In contrast to results based on actual field observations, considerably weaker coupling vertical strength was observed within SWAT open loop predictions. When simulated surface wetness was above average, surface and root-zone soil moisture variations were almost completely decoupled. As with the observations, relatively greater amount of coupling was found for dry soil moisture conditions – although the level of coupling was still less than that found in the observations. These wet/dry variations in vertical coupling strength, in turn, led to different EnKF performance based on surface wetness conditions. Overall, only the top layer under wetter conditions had satisfactory results as indicated by NSE (Table 4). However, improvement skill (NER) was notably better for the second and third layers in the drier surface conditions, due to their stronger coupling with surface layer. This suggests that overall better data assimilation results could be obtained if SWAT vertical coupling strength was increased (and made more in line with observations) through alternative subsurface water flow physics.

Although the EnKF was able to reduce some random stream flow errors in the synthetic twin experiment, such ability was impaired in the real-data environment because of the imperfect model representation of the true relationship between soil moisture and runoff generation (Fig. 6). In the open loop, Q_{gw} was severely underestimated (Fig. 5), which inferred suppressed recharge from deep percolation that is in turn, associated with positively-biased root-zone soil moisture. On the other hand, Q_{evt} was considerably

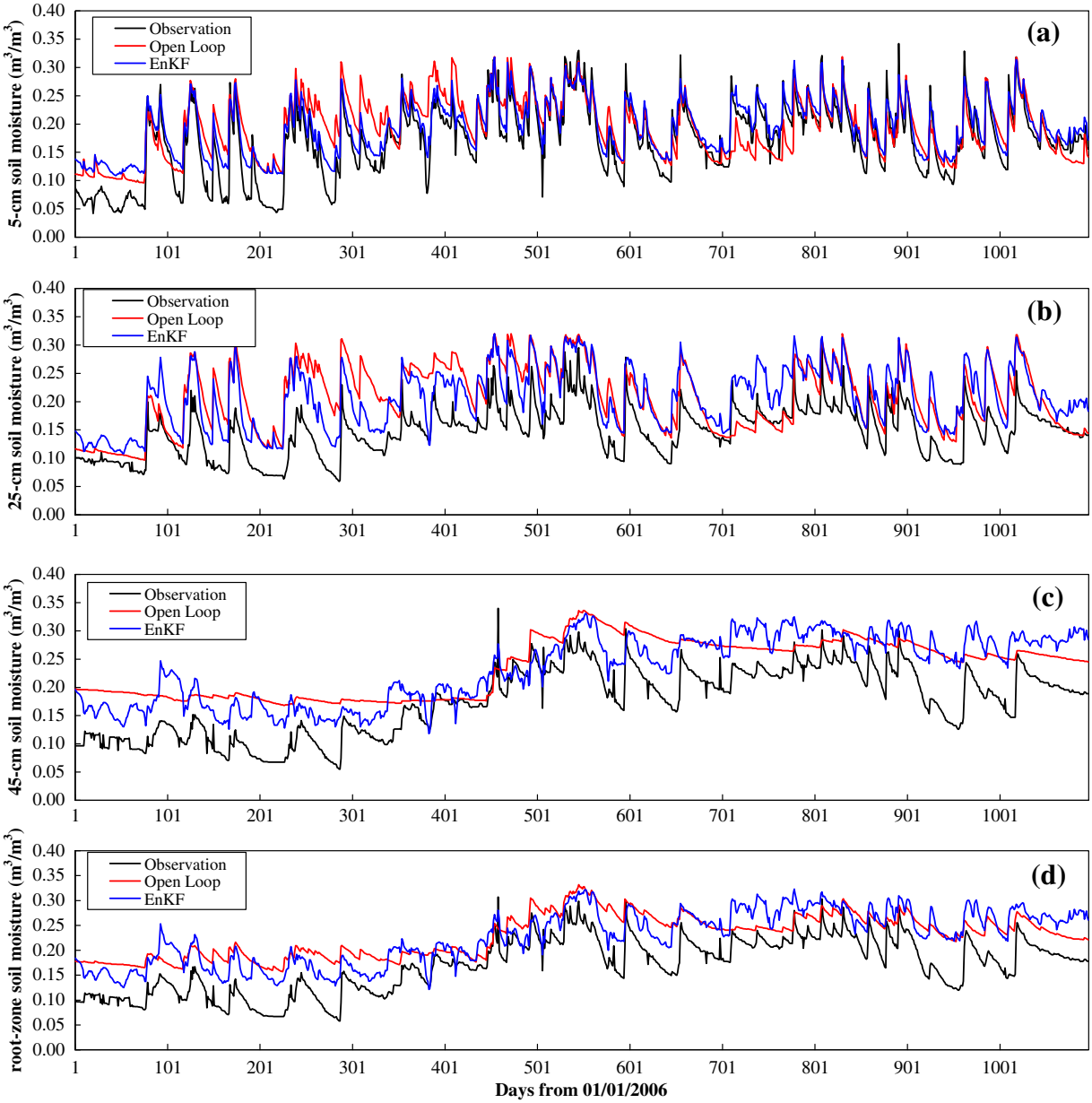

Fig. 4. Observed vs. open loop and real-data EnKF volumetric soil moisture.

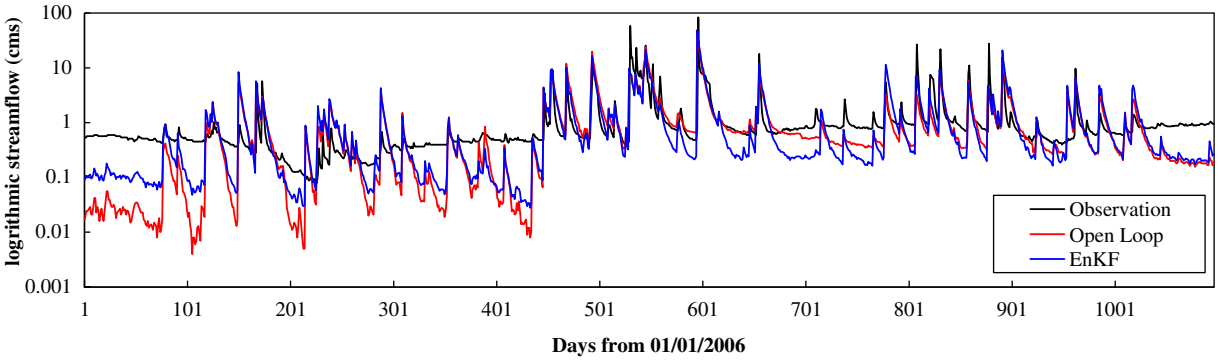

Fig. 5. Observed vs. open loop and real-data EnKF stream flow.

overestimated, especially during dry conditions. As noted above, the EnKF is not well-suited for correcting such biases. However, some of these problems could be addressed via a modified model calibration procedure. The biased flow components, for instance,

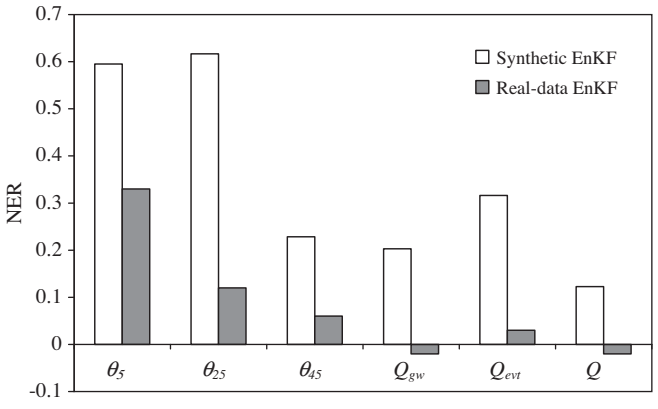

Fig. 6. Comparison of synthetic and real-data assimilation results. Synthetic EnKF results are the mean values of repeated experiments with maximum vertical error correlation as shown in Fig. 2.

Table 3
Summary of vertical coupling strengths. CR denotes Pearson product–moment correlation coefficient. Volumetric soil moisture values at 5, 25, 45 cm and root zone are denoted as $\theta_{5\text{-cm}}$, $\theta_{25\text{-cm}}$, $\theta_{45\text{-cm}}$, and θ_{rz}, respectively. Root zone includes soil profile from top to 130 cm. Wet or dry surface conditions refer to days on which surface soil moisture is above or below the average of the particular time-series.

	θ_5 vs. θ_{25}	θ_5 vs. θ_{45}	θ_{25} vs. θ_{45}	θ_5 vs. θ_{rz}
All conditions				
Observation	0.89	0.67	0.80	0.75
Open loop	0.97	0.11	0.14	0.41
EnKF	0.98	0.50	0.55	0.65
Wet surface conditions				
Observation	0.74	0.38	0.67	0.47
Open loop	0.87	0.05	0.18	0.19
EnKF	0.89	0.21	0.36	0.33
Dry surface conditions				
Observation	0.78	0.68	0.80	0.72
Open loop	0.96	0.34	0.32	0.50
EnKF	0.95	0.53	0.58	0.62

may be attributable to the higher sensitivity of the calibration metric (sum of square residuals) to the peak flow relative to the low-frequency signal of base flow. In a separate model calibration run based on log-transformed stream flow, Q_{gw} goodness-of-fit was greatly enhanced while event flow was consistently underestimated (not shown).

It is also possible that the performance of the EnKF was degraded via inappropriate model error assumptions (e.g. the auto-correlation, vertical cross-correlation and magnitude of model perturbations described in Section 2.5) [31]. Admittedly, the specification of these parameters was somewhat arbitrary. However, even synthetic EnKF results – based on a perfect statistical representation of modeling errors – demonstrated inconsistent stream flow results (Section 3.1). Consequently, it does not appear likely that real data results can be substantially improved via an alternative statistical parameterization of modeling errors.

4. Summary and discussion

A 1-D Ensemble Kalman filter was implemented on a semi-distributed hydrologic model (SWAT) to assimilate surface soil moisture observations and the updated hydrologic predictions were evaluated. This study was motivated by the availability of several existing and upcoming satellite surface soil moisture products that can be utilized to constrain root-zone soil water predictions (and potentially evapotranspiration and stream flow components) in a widely-used model within the agricultural and water resources management communities. Our synthetic twin study demonstrated EnKF can effectively update SWAT's upper-layer soil moisture and provide moderate improvement to the lower-layer soil moisture and evapotranspiration. EnKF analysis of flow-related variables was sensitive to the assumption about vertical error correlation. In general, assuming high vertical error correlations resulted in better prediction skill for flow components. While soil water improvements were relatively stable with given experiment specifications, analysis of deep percolation and hence groundwater flow showed considerable uncertainty, indicating inadequate model physics governing groundwater recharge along the lower boundary of the unsaturated zone.

Assimilation of actual surface soil moisture data had limited success in the upper layers only and was generally unsuccessful in improving stream flow prediction. To a large extent, SWAT open loop could reproduce the pattern of actual vertical coupling variations according to surface wetness, but the modeled coupling strength was significantly weaker than reality and complete decoupling occurred in some conditions. This decoupling limits the ability of the EnKF to update the soil moisture states of deeper layers. It should be noted that the assimilated soil moisture observations were based on unperturbed ground-observations rather than actual remote sensing retrievals and obtained at a slightly higher temporal frequency than satellite observations. Consequently, these results represented a best-case scenario that does not fully capture the impact of limitations in a remotely-sensed soil moisture product. It is instructive to note that, even with these optimistic assumptions concerning the quality and quantity of remotely-sensed surface soil moisture data, significant difficulties were encountered when updating deeper soil moisture and/or stream flow predictions. This suggests that vertical coupling issues in these models will have to be resolved before soil moisture data assimilation can be applied successfully.

In addition to vertical coupling issues, the failure of EnKF to substantially improve root-zone soil moisture and stream flow prediction is also partially attributable to suboptimal model calibration. Calibration for total stream flow resulted in heavily-biased

Table 4
Comparison of open loop and EnKF results for the real data assimilation experiment.

	Open loop						EnKF								
	NSE			Pbas			NSE			Pbas			NER		
	All	Wet	Dry	All	Wet	Dry	All	Wet	Dry	All	Wet	Dry	All	Wet	Dry
θ_5	0.48	−0.01	−0.99	13.1	2.2	36.5	0.77	0.73	−0.06	13.4	5.5	30.6	0.33	0.48	0.27
θ_{25}	−1.9	−4.79	−4.68	41.0	36.9	48.1	−1.24	−4.54	−1.89	40.6	41.4	39.2	0.12	0.02	0.29
θ_{45}	−0.31	0.02	−1.60	34.3	21.0	55.8	−0.16	−0.39	−0.71	32.4	25.6	43.5	0.06	−0.19	0.19
θ_{rz}	−0.41	−0.33	−1.87	34.6	23.0	53.9	−0.25	−0.82	−0.86	33.1	27.5	42.4	0.06	−0.17	0.19
Q	0.35	0.33	−3.04	−16.3	−12.8	−31.3	0.32	0.31	−4.62	−12.9	−6.8	−25.9	−0.02	−0.01	−0.05
Q_{gw}	−0.41	−0.49	−1.81	−76.2	−80.0	−67.6	−0.46	−0.55	−1.73	−76.4	−81.5	−65.2	−0.02	−0.02	0.01
Q_{evt}	0.2	0.19	−106.43	67.9	55.9	483.5	0.24	0.23	−124.87	71.8	58.8	519.9	0.03	0.03	−0.08

root-zone soil moisture, base flow and storm event flow which cannot be corrected by the EnKF. Alternative calibration using log-transformed stream flow may yield better background base flow prediction and possibly reduce the soil moisture bias through the percolation process and thus enhance the EnKF performance. However, it is likely that such improvement will be realized at the expense of peak stream flow predictions. Other techniques such as combined state-parameter estimation (e.g. [10]) may also provide a viable solution.

In closing, it should be acknowledged that the subsurface physics of SWAT are not designed to accurately reflect the vertical coupling between surface and subsurface soil moisture states. Our attempt to implement data assimilation techniques on the model represents a stretch beyond the applications for which SWAT was originally intended (and explicitly designed for). However, the structural model deficiencies prevented the EnKF-based assimilation of surface soil moisture from successfully constraining deep-layer soil moisture and subsequently groundwater flow (which relies on deep percolation) and surface runoff (which relies on profile soil water content). The presence of significant vertical coupling in profile soil moisture observations at the site suggests that better vertical physics in SWAT could lead to a better representation of profile soil moisture dynamics and substantially better soil moisture data assimilation results. Since such modifications may prove detrimental to other more established SWAT applications, a more reasonable approach might be the assimilation of root-zone (as opposed to surface zone) soil moisture products derived from either thermal infrared observations [32] or the microwave-bases surface soil moisture retrievals which have been temporally smoothed to capture slower root-zone dynamics [33].

Acknowledgements

This research was supported by a post-doctoral fellowship awarded by the USDA Agricultural Research Service and NASA grant NNH04AC3D1 (W.T. Crow – P.I.).

References

[1] Moradkhani H, Hsu KL, Gupta H, Sorooshian S. Uncertainty assessment of hydrologic model states and parameters: sequential data assimilation using the particle filter. Water Resour Res 2005;41:W05012.
[2] Reichle RH, McLaughlin DB, Entekhabi D. Hydrologic data assimilation with the ensemble Kalman filter. Mon Weather Rev 2002;130:103–14.
[3] Seo D, Koren V, Cajina N. Real-time variational assimilation of hydrologic and hydrometeorological data into operational hydrologic forecasting. J Hydrometeorol 2003;4:627–41.
[4] Evensen G. Data assimilation: the ensemble Kalman filter. Berlin: Springer; 2006.
[5] Reichle RH, Walker JP, Koster RD, Houser PR. Extended vs. ensemble Kalman filtering for land data assimilation. J Hydrometeorol 2002;3:728–40.
[6] Aubert D, Loumagne C, Oudin L. Sequential assimilation of soil moisture and streamflow data in a conceptual rainfall–runoff model. J Hydrol 2003;280:145–61.
[7] Clark MP, Rupp DE, Woods RA, Zheng X, Ibbitt RP, Slater AG, et al. Hydrological data assimilation with the ensemble Kalman filter: use of streamflow observations to update states in a distributed hydrological model. Adv Water Res 2008;31:1309–24.
[8] Crow WT, Ryu D. A new data assimilation approach for improving runoff prediction using remotely-sensed soil moisture retrievals. Hydrol Earth Syst Sci 2009;13:1–16.
[9] Komma J, Blöschl G, Reszler C. Soil moisture updating by ensemble Kalman Filtering in real-time flood forecasting. J Hydrol 2008;357:228–42.
[10] Xie XH, Zhang DX. Data assimilation for distributed hydrological catchment modeling via ensemble Kalman filter. Adv Water Res 2010;33:678–90.
[11] Kerr YH, Levine D. Forward to the special issue on the Soil Moisture and Ocean Salinity (SMOS) mission. IEEE Trans Geosci Remote Sens 2008;46:583–5.
[12] Entekhabi D, Njoku E, O'Neill P, Kellogg K, Crow WT, Edelstein W, et al. The Soil Moisture Active and Passive (SMAP) mission. IEEE Proc 2010;98:704–16.
[13] Arnold JG, Srinivasan R, Muttiah RS, Williams JR. Large area hydrologic modeling and assessment. Part I: model development. J Am Water Res Assoc 1998;34:73–89.
[14] Neitsch SL, Arnold JG, Kiniry JR, Srinivasan R, Williams JR. Soil and water assessment tool theoretical documentation, version 2005. [internet]. 2005 Jan [cited 2010 Aug 12]; Available from: <http://swatmodel.tamu.edu/media/1292/SWAT2005theory.pdf>.
[15] Gassman PW, Reyes MR, Green CH, Arnold JG. The Soil and Water Assessment Tool: historical development, applications and future research directions. Trans Am Soc Agric Biol Eng 2007;50:1211–50.
[16] Crow WT, Wood EF. The value of coarse-scale soil moisture observations for regional surface energy balance modeling. J Hydrometeorol 2002;3:467–82.
[17] Margulis SA, McLaughlin D, Entekhabi D, Dunne S. Land data assimilation of soil moisture using measurements from the Southern Great Plains 1997 field experiment. Water Resour Res 2002;38:1299.
[18] Kumar SV, Reichle RH, Koster RD, Crow WT, Peters-Lidard CD. Role of subsurface physics in the assimilation of surface soil moisture observations. J Hydrometeorol 2009;10:1534–47.
[19] Li F, Crow WT, Kustas WP. Towards the estimation of root-zone soil moisture via the simultaneous assimilation of thermal and microwave soil moisture retrievals. Adv Water Res 2010;33:201–14.
[20] Evensen G. Sequential data assimilation with a nonlinear quasi-geostrophic model using Monte Carlo methods to forecast error statistics. J Geophys Res 1994;99:143–62.
[21] Burgers G, van Leeuwen PJ, Evensen G. Analysis scheme in the ensemble Kalman filter. Mon Weather Rev 1998;126:1719–24.
[22] Jensen ME, Burman RD, Allen RG. Evapotranspiration and irrigation water requirements. ASCE manuals and reports on engineering practice No. 79. New York: ASCE; 1990.
[23] Tripp DR, Niemann JD. Evaluating the parameter identifiability and structural validity of a probability-distributed model for soil moisture. J Hydrol 2008;353:93–108.
[24] Starks PJ, Moriasi DN. Spatial resolution effect of precipitation data on SWAT calibration and performance: implications for CEAP. Trans ASABE 2009;52:1171–80.
[25] Duan QY, Sorooshian S, Gupta VK. Optimal use of the SCE-UA global optimization method for calibrating watershed models. J Hydrol 1994;158:265–84.
[26] Reichle RH, Koster RD. Global assimilation of satellite surface soil moisture retrievals into the NASA Catchment land surface model. Geophy Res Lett 2005;32:L02404.
[27] Arnold JG, Allen PM. Automated methods for estimating baseflow and ground water recharge from streamflow records. Am Water Res Assoc 1999;35:411–24.
[28] Nash JE, Sutcliffe JV. River flow forecasting through conceptual models. Part 1: a discussion principles. J Hydrol 1970;10:282–90.
[29] McCuen RH, Knight Z, Cutter AG. Evaluation of the Nash–Sutcliffe efficiency index. J Hydrologic Eng 2006;11:597.
[30] Moriasi DN, Arnold JG, Van Liew MW, Bingner RL, Harmel R, Veith TL. Model evaluation guidelines for systematic quantification of accuracy in watershed simulations. Trans ASABE 2007;50:885–900.
[31] Crow WT, Van Loon E. The impact of incorrect model error assumptions on the sequential assimilation of remotely sensed surface soil moisture. J Hydrometeorol 2006;8:421–31.
[32] Crow WT, Kustas WP, Prueger J. Monitoring root-zone soil moisture through the assimilation of a thermal remote sensing-based soil moisture proxy into a water balance model. Remote Sens Environ 2008;112:1268–81.
[33] Albergel C, Rüdiger C, Pellarin T, Calvet J-C, Fritz N, Froissard F, et al. From near-surface to root-zone soil moisture using an exponential filter: an assessment of the method based on in-situ observations and model simulations. Hydrol Earth Syst Sci 2008;12:1323–37.